A spectral model for sudden dissipation effect in turbulent plasma under compression

G. Viciconte [a], B.-J. Gréa [b], F. S. Godeferd[c]

a. CEA, DAM, DIF, F-91297 Arpajon, France
LMFA, UMR5509, Ecole Centrale de Lyon, 69131 Ecully cedex, France
giovanni.viciconte@cea.fr
b. CEA, DAM, DIF, F-91297 Arpajon, France
benoit-joseph.grea@cea.fr
c. LMFA, UMR5509, Ecole Centrale de Lyon, 69131 Ecully cedex, France
fabien.godeferd@ec-lyon.fr

Résumé :

Les plasma turbulents en régime cinétique et soumis à une compression peuvent voir leur énergie cinétique subitement dissipée suite à la forte augmentation de la viscosité avec la croissance de la température [1]. Un modèle statistique spectral utilisant une fermeture isotrope de type Eddy Damped Quasi Normal Markovian (EDQNM) est proposé pour analyser ce phénomène. Le modèle est comparé et validé par des données de simulation numerique directe (DNS) portant sur les statistiques en un point et les spectres de corrélation à deux points. Nous étudions ainsi l'équilibre entre la production de turbulence due à la compression et les effets de dissipation amplifiés par la croissance de la viscosité, dans un régime à haut nombre de Reynolds non atteignable par la DNS. L'influence des conditions initiales sur l'évolution de l'énergie cinétique est ensuite examinée.

Abstract :

Turbulent plasmas under compression and entering the kinetic regime can experience a sudden increase of kinetic energy dissipation due to an abrupt growth of the viscosity from temperature increase [1]. A statistical spectral model based on isotropic Eddy Damped Quasi Normal Markovian (EDQNM) closures [2] is proposed to analyse this phenomenon. The model is validated and compared against Direct Numerical Simulations (DNS) results providing one point turbulent statistics and two-point correlation spectra. Thanks to the model, in the high Reynolds number regime unreachable by DNS, we explore the balance between turbulence production due to compression and enhanced dissipation due to the viscosity growth. We also examine the influence of initial conditions on turbulent kinetic energy evolution.

Mots clefs : Compressed turbulence, plasma effect, EDQNM, Direct Numerical Simulation.

1 Introduction

In inertial confinement fusion (ICF), hydrodynamic instabilities generated by the compression of the capsule can eventually lead to a turbulent state [3]. Simultaneously, the different materials experience a tremendous increase of temperature until becoming a plasma. When entering the kinetic regime, the plasma viscosity increase leads to a sudden dissipation of turbulent kinetic energy (TKE) [1]. This effect is difficult to predict since it involves several concurrent phenomena, but it may influence significantly the mixing and consequently the capsule yield.

In order to measure the importance of this phenomenon and its sensitivity to different parameters, we propose a spectral model of turbulence under compression based on classical EDQNM closures. This strategy is complementary to DNS as it allows parametric studies and to explore high Reynolds numbers due to its low computational cost. It has been successfully used in many applications including rotating turbulence, stably or unstably stratified turbulence [4, 5]. An important question we address here is the influence of initial conditions on the flow development. Indeed, the distribution of initial energy at large scales has been recognized to play a determinant role in the dynamics of other turbulent flows such as the decay of homogeneous isotropic turbulence HIT [6] or unstably stratified turbulence [7].

This paper is organized as follows : First we present the basic equations and a statistical model for the fluctuating turbulent quantities submitted to compression. Then we validate the model against DNS data of [1] and our new simulations at higher resolution. Finally, we analyse the influence of initial conditions on the sudden dissipation phenomenon at higher Reynolds number.

2 Basic equations

In this section, we introduce the theoretical framework and the model for turbulence under compression. In section 2.1, we present the coordinate transformation and the scaling law allowing us to follow turbulent quantities in the moving frame attached to the mean flow. In section 2.2 we derive the statistical EDQNM model.

2.1 Equation for modelling compression

We consider the isotropic compression of a turbulent plasma in the zero Mach number limit. Following [8, 1], turbulent fluctuations are thus assumed incompressible. The size of the domain as a function of time is characterized by the length $\bar{L}(t)$ which is non dimensionalized as $L(t) = \bar{L}/L_0$ using the initial dimension L_0 of the domain. Introducing the compression rate V_b, we assume that $L(t)$ varies linearly with time as $L(t) = 1 - 2V_b t$.

The equation governing the incompressible fluctuating velocity $\mathbf{u}$ is [8] :

$$\partial_t \mathbf{u} + \mathbf{u} \cdot \nabla \mathbf{u} + A\mathbf{x} \cdot \nabla \mathbf{u} + A\mathbf{u} = -\frac{1}{\bar{\rho}} \nabla p + \frac{\mu}{\bar{\rho}} \nabla^2 \mathbf{u}, \tag{1}$$

with p the fluctuation pressure, $\bar{\rho}$ the mean density and μ the viscosity coefficient. This equation comes from the Navier-Stokes equation for a compressible flow where the classical Reynolds decomposition into mean and fluctuating parts has been introduced. In addition, the mean velocity $\bar{\mathbf{u}} = A(t)\mathbf{x}$ is related to the domain size by the mass conservation as $\bar{\rho} \sim L^{-3}$ leading to $A(t) = \dot{L}/L$ (the overdot indicates time-derivation).

Equation (1) contains an inhomogeneous term $A\mathbf{x}\cdot\nabla\mathbf{u}$ with an explicit dependence on space coordinate. For simplification, it is convenient to do a change of coordinates into the moving frame attached to the background flow, using $L(t)^{-1}\mathbf{x}=\hat{\mathbf{x}}$, so that fluctuations can be assumed homogeneous in the new coordinates $\hat{\mathbf{x}}$. Accordingly, Equation (1) becomes

$$\partial_t\mathbf{u}+\frac{1}{L}\mathbf{u}\nabla\mathbf{u}+\frac{\dot{L}}{L}\mathbf{u}=-\frac{L^2}{\rho_0}\nabla p+\frac{L\mu(T)}{\rho_0}\nabla^2\mathbf{u}\ . \tag{2}$$

In the moving frame, compression effects thus appear through a forcing (or damping) term $\dot{L}/L\mathbf{u}$ and a time-dependent coefficient in front of advective, pressure and viscous terms. In order to simplify further the problem, velocity, pressure and time can be rescaled as

$$\hat{\mathbf{u}}(\hat{\mathbf{x}},\tau)=L(t)^{\alpha}\mathbf{u}(\hat{\mathbf{x}},t) \tag{3a}$$

$$\hat{p}(\hat{\mathbf{x}},\tau)=L(t)^{2+\alpha-\gamma}p(\hat{\mathbf{x}},t) \tag{3b}$$

$$d\tau=L(t)^{\gamma}dt \tag{3c}$$

leading to

$$\frac{\partial\hat{\mathbf{u}}}{\partial\tau}+L^{-\alpha-\gamma-1}\hat{\mathbf{u}}\cdot\nabla\hat{\mathbf{u}}+L^{-\gamma-1}\dot{L}\hat{\mathbf{u}}(1-\alpha)=-\frac{1}{\rho_0}\nabla\hat{p}+\frac{L^{1-\gamma}\mu(T)}{\rho_0}\nabla^2\hat{\mathbf{u}}\ . \tag{4}$$

The relation between the size of the compressing domain and the temperature is established thanks to the hypothesis of adiabatic compression of ideal monoatomic gas. Temperature evolves as

$$T(t)=T_0\left(L_0/L(t)\right)^2$$

and viscosity in the plasma as

$$\mu(t)=\mu_0\left(T_0/T(t)\right)^{\beta}$$

such that the viscosity as a function of $L(t)$ is [1],

$$\mu=\mu_0 L(t)^{-2\beta}\ .$$

In the case of a plasma in the kinetic regime, $\beta=5/2$.

In Equation 4, we impose that the coefficient corresponding to the non linear advection term is constant, giving $\alpha+\gamma=-1$. This can be used in two ways :

1. It is possible to eliminate the forcing term by choosing $\alpha=1$, leading to a regular Navier-Stokes equation with a time dependent viscosity.
2. One can keep a constant viscosity coefficient with $\alpha=3$, and finally have a Navier-Stokes equation with a time dependent forcing term.

These two different choices provide two different equations that model the same phenomenon. In [1], the authors have chosen the second option. In section 2.2, we derive the EDQNM model for both cases.

2.2 Statistical approach : EDQNM Model

The EDQNM (Eddy damped quasi-normal markovian) closure has proven an efficient closure for different types of turbulent flows. The first EDQNM model concerned isotropic turbulence, in which a damping timescale $(\Theta_{kpq})^{-1}$ was used to adjust non linear decorrelation of the third-order cumulants generating the exchange of energy between three wavenumbers k, p, q (see *e.g.* [6]). More or less sophisticated extensions of the EDQNM model were proposed to account for additional distorsions to turbulence : mean velocity gradients, buoyancy force for stratified flows, Lorentz-Laplace force in magnetohydrodynamics, Coriolis force for rotating flows. [5] In short, when accounting for such additional forcing in the Navier-Stokes equation, one can account for the corresponding linear term at different levels of the closure (namely, choosing to retain its influence on increasingly higher order statistics, *e.g.* second- or third-order statistical moments). Since we deal with a rather strong effect of the additional linear terms arising in Equation (4), we anticipate that its direct effect on non linear transfers will be second-order in amplitude with respect to its direct effect on energy spectra, and we retain a simple version of the EDQNM closure, in which spectral energy transfers $T(k)$ will be closed with the same rationale as for isotropic turbulence. We shall see in section 3 that the resulting model compares very well with DNS.

Therefore, in the following, we derive the EDQNM closure for the compressed turbulence with plasma effect, for each of the two above-mentioned options for behaviour equations.

2.2.1 First case : Time-dependent viscosity

Eliminating the forcing term ($\alpha = 1$ and $\gamma = -2$) in Equation (4) we obtain

$$\partial_\tau \hat{\mathbf{u}} + \hat{\mathbf{u}} \cdot \nabla \hat{\mathbf{u}} = -\nabla \hat{p} + \nu_0 L^{-2} \nabla^2 \hat{\mathbf{u}} \tag{5}$$

where $L(\tau) = 1/(1 + 2V_b\tau)$. It is then clear that, when t goes to infinity, the dissipation term in Eq. (5) tends to infinity as well, thus causing the sudden dissipation of kinetic energy. As done for the classical Navier-Stokes equation, one can derive the two-point velocity correlation evolution equation from Eq. (5), and derive the evolution equation for the two-point velocity spectrum and then obtain the Lin equation for the kinetic energy spectrum $E(k)$.

In the present case, the corresponding dynamical equation for the kinetic energy spectrum is

$$\partial_\tau E(k,\tau) + 2\nu_0 (1 + 2V_b\tau)^2 k^2 E(k,\tau) = T(k,\tau) \tag{6}$$

where the energy transfer term $T(k,\tau)$ is closed using the classical EDQNM closure

$$T(k,\tau) = \iint_{\Delta_k} \Theta_{kpq} \frac{k}{pq} E(q,\tau) b(k,p,q) \left(k^2 E(p,\tau) - p^2 E(k,\tau)\right) \mathrm{d}p\mathrm{d}q \ . \tag{7}$$

$b(k,p,q)$ is the classical geometrical coefficient related to the geometry of the triad [5] and Θ_{kpq} is the characteristic time appearing during the combined markovianization and eddy-damping process.

Its expression is thus provided by

$$\Theta_{kpq}(\tau) = \frac{1 - e^{\mu_{kpq}\tau + (1+2V_b\tau)^2\nu_0(k^2+\nu p^2+\nu q^2)\tau}}{\mu_{kpq} + (1+2V_b\tau)^2\nu_0(k^2+\nu p^2+\nu q^2)} \tag{8}$$

$$\text{with } \mu_{kpq} = \nu_k + \nu_p + \nu_q \text{ and } \nu_k = 0.36\left(\int_0^k p^2 E(p)dp\right)^{1/2} .$$

2.2.2 Second case : Forcing term

Eliminating the time dependencies in front of the viscosity term of Equation (4) ($\alpha = 3$ and $\gamma = -4$), we obtain

$$\partial_\tau \hat{\mathbf{u}} + \hat{\mathbf{u}} \cdot \nabla \hat{\mathbf{u}} - 2\dot{L}L^3\hat{\mathbf{u}} = -\nabla\hat{p} + \nu_0\nabla^2\hat{\mathbf{u}} \tag{9}$$

with $L(\tau) = 1/\sqrt[3]{1+6V_b\tau}$. The corresponding Lin equation for this case reads

$$\left(\partial_\tau + 2\nu_0 k^2\right) E(k,\tau) = T(k,\tau) - D(\tau)E(k,\tau) \tag{10}$$

where $D(\tau) = -2\dot{L}L^3 = 4V_b/(1+2V_b\tau)$. The energy transfer term $T(k,\tau)$ is the same as in the previous case, with the only difference in the detailed expression of Θ_{kpq} :

$$\Theta_{kpq}(\tau) = \frac{1 - e^{\mu_{kpq}\tau + \nu_0(k^2+\nu p^2+\nu q^2)\tau}}{\mu_{kpq} + \nu_0(k^2+\nu p^2+\nu q^2)} . \tag{11}$$

3 Validation

We now present comparisons between EDQNM results and results of DNS. We use DNS data from [1] simulations using 128^3 grid points, and from our own simulations using 256^3 grid points. In both cases, the initial Reynolds number is $Re_0 = 3000$. A close comparison permits to validate the closure and confirm that the statistical approach can later be used for an extensive parametric study. In addition, comparing the different DNS data permits to evaluate the influence of a modification of numerical parameters on DNS statistics.

The numerical integration of EDQNM model Equations (6) or (10) is done using a simple trapezoidal integration quadrature as regards the integral appearing in the transfer $T(k)$. Time-marching is done using a third-order strong stability preserving Runge-Kutta method, a treatment which we believe is original for solving these Lin-type equations. This scheme permits the use of larger time step with respect to the first-order Euler time-integration method used in previous works.

Our DNS are performed using a classical pseudo-spectral method (see [2]) in a three-dimensional 2π-periodic domain, and by considering a uniform viscosity with the only modification due to compression effects. The DNS code therefore computes the solution of Equation (5) with time varying viscosity.

Whereas statistics obtained in DNS is but a by-product of the velocity field for a particular realisation, obtained by averaging over the computational domain, the resolution of EDQNM equations directly provides the two-point statistics that can be simply integrated in order to obtain one-point statistics such as total kinetic energy. These statistics stand for the ensemble averaging that should be done if many DNS realization could be afforded. Therefore, when comparing DNS and EDQNM, one needs to bear in mind these differences between the two approaches. In addition, initial conditions in

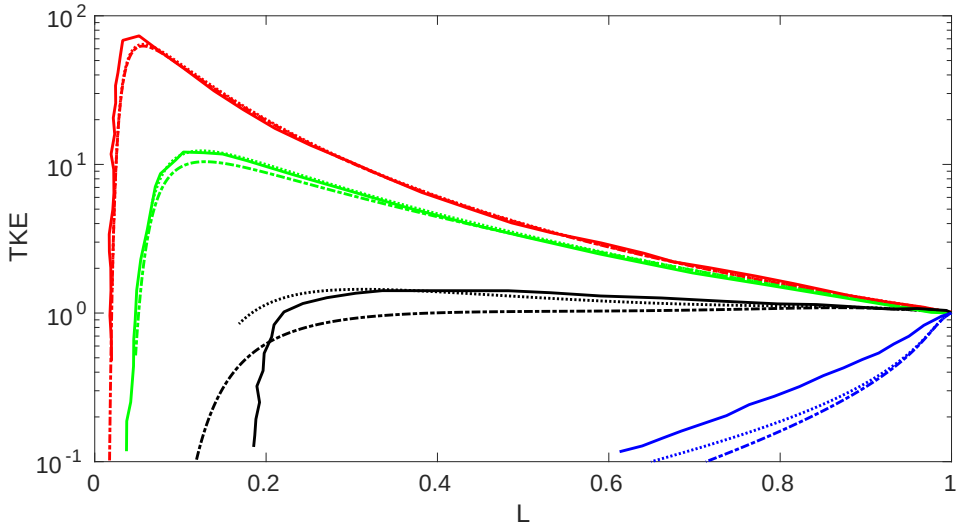

FIGURE 1 – Turbulent kinetic energy evolution as a function of domain size L. Solid lines : DNS results from Davidovits et al. Dotted lines : EDQNM forcing term closure. Dash-dotted lines : EDQNM time-dependent viscosity closure. Different colors for decreasing compression rates : red : $V_b = 100$; green :$V_b = 10$; black :$V_b = 1$; blue :$V_b = 0.1$.

DNS use fields that are δ-correlated, thus with zero third-order correlations. This is not the case in EDQNM in which energy transfers are immediately triggered at the beginning of the computation, and therefore have non zero values from the start.

Comparison with DNS of Davidovits *et al.* The time evolution of kinetic energy is shown in Figure 1 as a function of L, at different compression rates V_b. The figure presents results from the EDQNM model and from DNS by [1]. The initial kinetic energy is set to unity, and the time evolution goes from right to left, starting at the domain size $L = 1$.

The figure shows that kinetic energy evolution initially increases for compression rate V_b larger than 1, and decreases for $V_b < 1$. It then undergoes a sudden drop, triggered at a value of L increasing with V_b. This drop is not observed for $V_b = 0.1$ since kinetic energy decays too fast from the beginning.

Figure 1 also shows that EDQNM results agree very well with DNS data for $V_b > 1$. When $V_b \leq 1$ the curves depart slightly, but the overall trend is rather good. Such differences can be due to various factors :

1. slight differences in initial conditions (that are not fully detailed in [1]) ;
2. the effect of confinement at low-wave number, when the computational domain is too small in DNS, so that DNS simulation over a 128^3 grid is under-resolved initially, although this resolution rapidly becomes adequate when viscosity increases ;
3. there are differences between the two formulations of the model, based either on the time-dependent viscosity closure or on the forcing term closure. Although the two formulations should be formally equivalent, their numerical implementation can induce departures, as observed on the figure.

Comparison with new DNS data In order to have a better control of the parameters of the simulations we have therefore performed new Direct Numerical Simulations with known initial conditions,

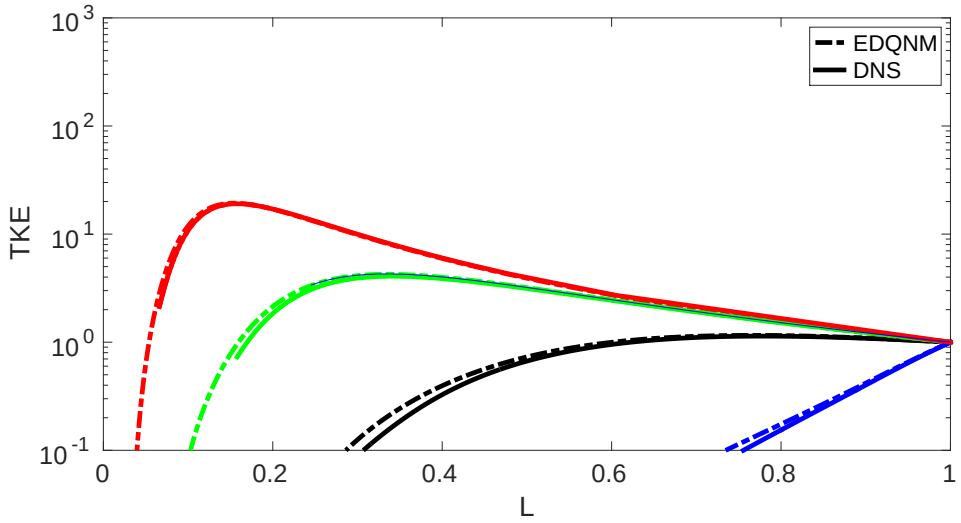

FIGURE 2 – Turbulent kinetic energy evolution as a function of domain size L. Solid lines : DNS results. Dash-dotted line : EDQNM time-dependent viscosity closure. Different colors for different compression rates : red :$V_b = 100$; green :$V_b = 10$; black :$V_b = 1$; blue :$V_b = 0.1$. Viscosity coefficient $\nu = 5 \times 10^{-2}$ in all simulations.

and increased resolution 256^3. This permits further validation and comparison of the EDQNM model results with those of our own DNS data, shown in Figure 2.

The initial energy spectrum is of the Von Karman type $E(k, t = 0) \propto k^4 \exp\left[-2\,(k/k_{peak})^2\right]$ with a peak wavenumber $k_{peak} = 4$.

For the large compression rates $V_b \geq 10$, Figure 2 shows an almost perfect agreement between EDQNM and DNS kinetic energy evolution, better than in Figure 1. In addition, the agreement is also much improved for the lesser compression rates V_b. This is the result of the increase of resolution in the DNS, and of better controlled initial conditions as well.

Figure 3 shows the evolution of the compressed flow at decreasing domain size $L = 1$, 0.6, 0.3 and 0.16.

Figures 3a, 3c, 3e, 3g show the three-dimensional distribution of kinetic energy in the turbulent box. As the compression proceeds, the energy-containing eddies appear to grow both in extension and intensity, which is maximal in the $L = 0.3$ case, that indeed corresponds to the peak of kinetic energy in Figure 2 for $V_b = 10$. When the turbulent kinetic energy achieves its maximum value, the dissipation effect starts to influence not only the small scales but also the bigger ones. As expected, later on, the high energy structures are dissipated by viscosity, and the flow in Figure 3g is clearly much less energetic.

Figures 3b, 3d, 3f, 3h present the comparison between energy spectra from DNS and from EDQNM at times corresponding to the above-discussed distributions of kinetic energy. The initial spectrum shown in Figure 3b is used by both DNS and EDQNM, so that the two spectra exatly collapse. At decreasing L, the DNS and EDQNM spectra begin to depart mostly in the high wavenumber range, as shown in Figures 3d and 3f, with EDQNM energy smaller than in DNS. The kinetic energy distribution for large-scale structures at small wavenumbers continues to agree very well until $L = 0.3$. However, when the dissipation effect surge occurs (Figure 3h), the departure extends to the low wave number range. Interestingly, while energy at high wavenumbers is lower in EDQNM with respect to DNS,

it is larger in the small wavenumber range. Up to this point, it is hard to tell whether numerical confinement in DNS or model imperfection are accountable for the differences. Overall, in view of these comparisons, the EDQNM model predictions are nonetheless very good throughout the complete spectral range and time evolution.

4 Sensitivity to initial conditions

In this section, we present the analysis of compressed turbulence at higher Reynolds number than in the above cases, thanks to the capacity of the EDQNM model to represent highly energetic turbulence for several parameters. Our objective here is to shed light on the importance of initial conditions onto the evolution of the flow.

Two types of the initial conditions are therefore considered with the same kinetic energy, and same integral length scale expressed as :

$$\ell_I \sim \frac{\int_0^\infty k^{-1} E(k,t) dk}{\int_0^\infty E(k,t) dk} \ . \tag{12}$$

The difference lies in the distribution of energy at large scales, namely the scaling $E(k) \sim k^s$ as $k \ll 1$. Here Batchelor $s = 4$ and Saffman $s = 2$ turbulence are considered with an initial turbulent Reynolds number of $Re = 2 \times 10^5$. The evolution of total kinetic energy with L for the two cases is presented in Figure 4 for different compression rates. When the dynamics is dominated by the turbulence production due to compression *i.e* at the beginning of the implosion ($L \sim 1$), the initial conditions do not influence the evolution of kinetic energy, and both Saffman and Batchelor cases result in the same level of kinetic energy during all the evolution. No difference at all can be observed for the larger compression rate $V_b = 100$. However, when the non linear and viscous effects become important, the two initial conditions lead to different paths, with differences both in the level of energy but also in the location of its maximum. This departure is clearly amplified at decreasing compression rate, the case at V_b exhibiting a separation of the Batchelor and Saffman cases as early as $L \simeq 0.2$, even before the maximum is reached. More precisely, it appears clearly that dissipation is smaller is the case $s = 2$ as the energy is more distributed at larger scales.

We now analyse this phenomenon in detail by identifying different decay regimes during the compression.

Self-similar turbulence decay regime Figure 4 demonstrates that initial condition obviously influence the self similar regime and the final period of decay of kinetic energy.

In the moving reference frame, turbulence may decay self-similarly following

$$\hat{K}(\tau) \sim \tau^{-n} \ , \tag{13}$$

and the decay exponent can be classically related to the slope of infrared spectra as (see [6]) :

$$n = \frac{2(s+1)}{s-3} \ . \tag{14}$$

This provides the decay exponent $n = 10/7 \simeq 1.43$ for Batchelor spectrum and $n = 6/5 = 1.2$ for Saffman spectrum. Returning to the laboratory frame, this leads to significant differences of kinetic

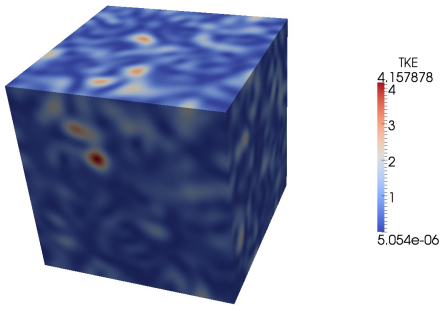

(a) Contour of kinetic energy at $L = 1$

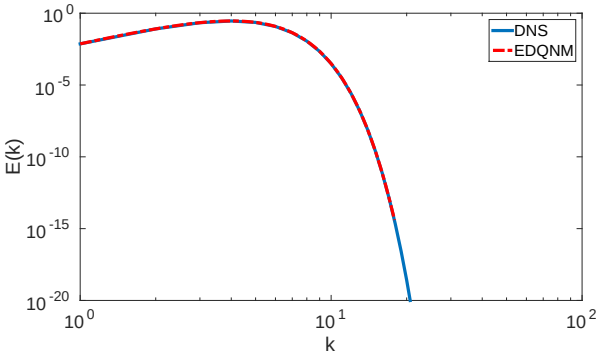

(b) Energy spectra at $L = 1$

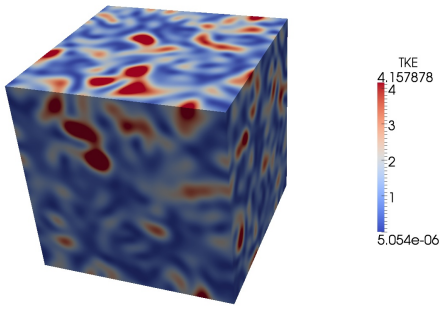

(c) Contour of kinetic energy at $L = 0.6$

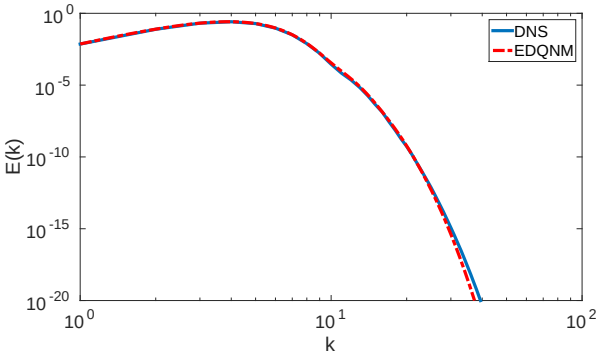

(d) Energy spectra at $L = 0.6$

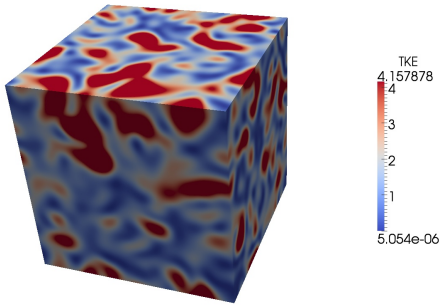

(e) Contour of kinetic energy at $L = 0.3$

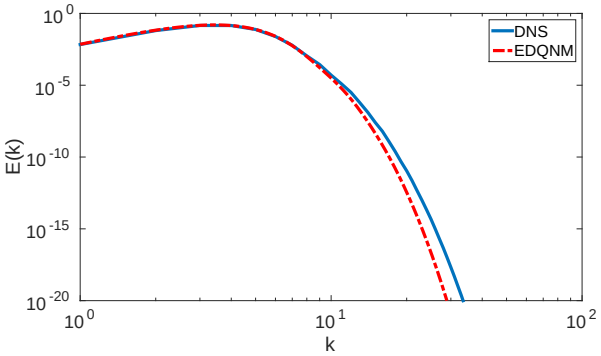

(f) Energy spectra at $L = 0.3$

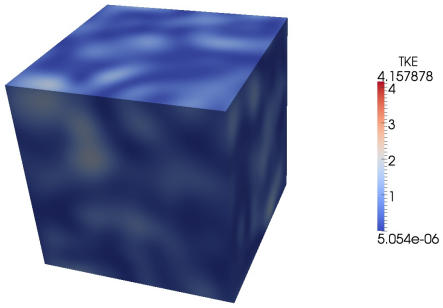

(g) Contour of kinetic energy at $L = 0.16$

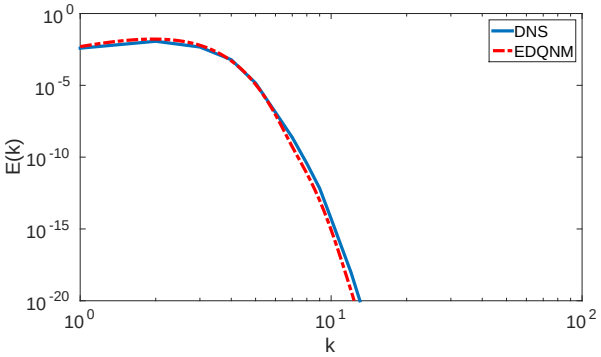

(h) Energy spectra at $L = 0.16$

FIGURE 3 – Left figures : contours of kinetic energy at decreasing domain size L ; right figures : corresponding kinetic energy spectra. The compression rate is $V_b = 10$.

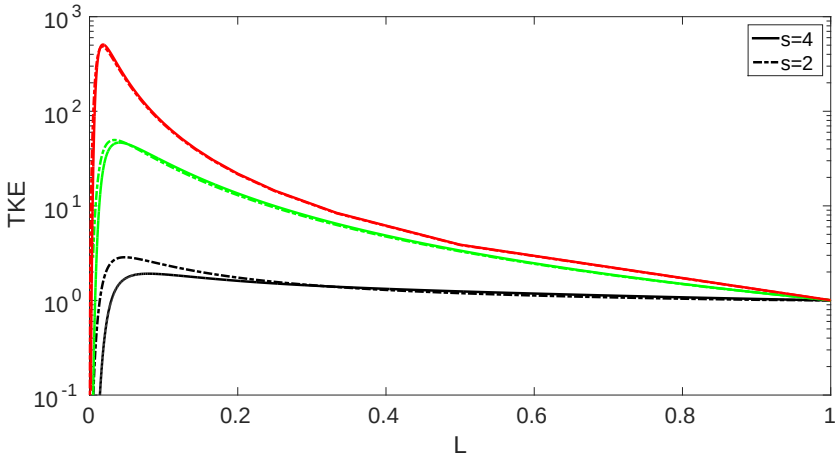

FIGURE 4 – Turbulent kinetic energy evolution as function of domain size, for initial conditions corresponding to Batchelor turbulence (infrared spectrum powerlaw k^4, solid lines) and Saffman turbulence (k^2, dashed lines), at different compression rates : red :$V_b = 100$; green :$V_b = 10$; black :$V_b = 1$.

energy evolution, since for $L \to 0$:

$$K \sim L^{n-2} \ . \tag{15}$$

We tested these predictions using the EDQNM model to predict the long time evolution of a very high Reynolds number flow in compression without plasma effect. Figure 5 shows the corresponding kinetic energy evolution. Starting from $L(t) = 1$, the evolution follows a L^{-2} law at short times, corresponding to the predictions of Rapid Distortion Theory which assumes that turbulence is "frozen" over the rapid timescale of the applied distorsion (here, the compression). After a short transient at about $L \simeq 0.02$, as L approaches zero, kinetic energy evolves according to the predicted scaling of Equation (15), corresponding to the self-similar decay regime of compressed turbulence. This is very clearly shown in Figure 5 by the EDQNM model, and would be much more difficult to observe in mere DNS.

Self-similar final decay regime We now consider the final period of decay of turbulence when the dynamics of the energy spectrum is driven by viscous effects. This phase corresponds to the sudden dissipation effects observed in the simulations. Again, it is possible to find self-similar solutions for these phases leading to the kinetic energy scaling

$$\hat{K}(\tau) \sim \tau^{-3(1+s)/2} \tag{16}$$

in the moving reference frame. In the laboratory reference frame, this translates into

$$K \sim L^{(3s-1)/2} \tag{17}$$

This equation shows that the smaller the infrared powerlaw of the spectrum, the slower the decay of kinetic energy with L. We therefore expect Saffman turbulence decay to be slower than Batchelor turbulence decay. Figure 6 illustrates this, and shows the behaviour of the turbulent kinetic energy during the sudden dissipation phase.

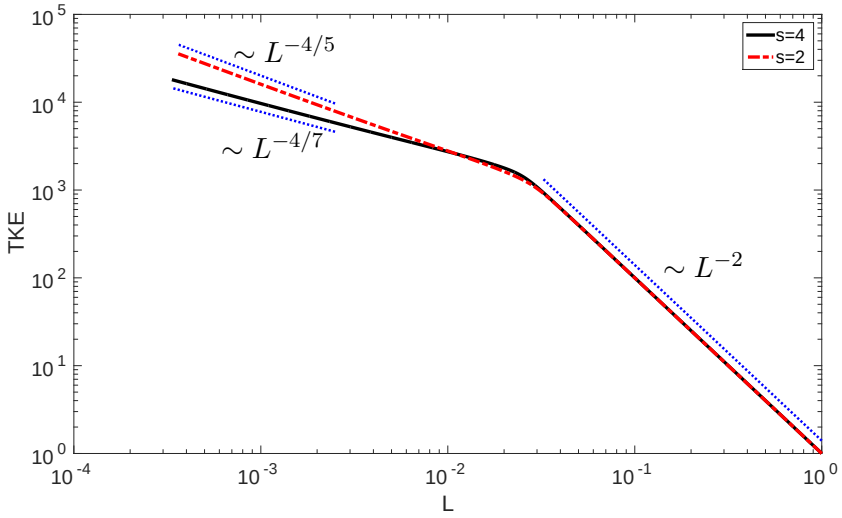

FIGURE 5 – Turbulent kinetic energy as function of $L(t)$, in case of compression without plasma effect. In this case there is not a sudden dissipation effect and the TKE continues to increase when $L(t)$ approaches 0. Initial conditions corresponding to Batchelor spectrum ($s = 4$) and Saffman spectrum ($s = 2$) are shown. EDQNM simulation at $Re = 2 \times 10^6$.

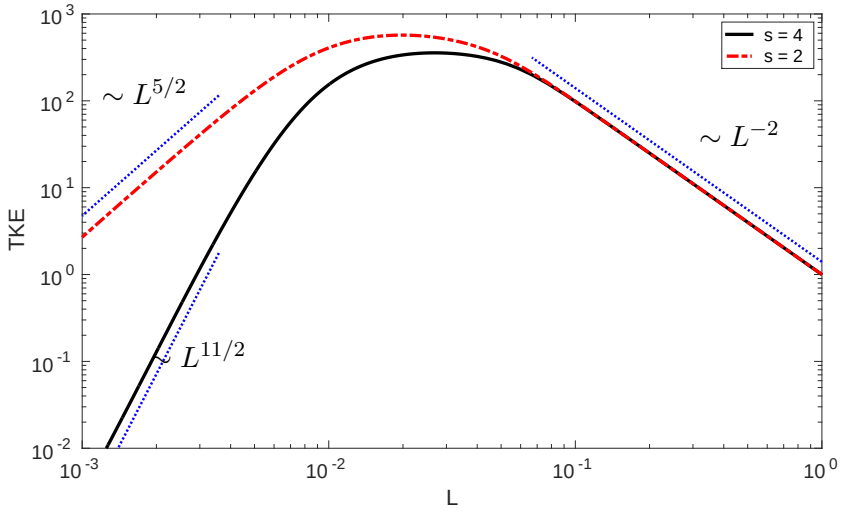

FIGURE 6 – Turbulent kinetic energy as function of $L(t)$, in the case of compression with plasma effect. Batchelor and Saffman turbulence at $s = 4$ and $s = 2$ infrared powerlaw are presented. EDQNM simulations at $Re = 2 \times 10^8$.

The figure clearly shows that the relaminarization phase depends strongly on the infrared scaling of the initial energy spectrum. Moreover, the asymptotic evolution at small L is very well described by Equation (17). In addition, since the scaling laws are very different between Saffman and Batchelor turbulence ($L^{11/2}$ vs $L^{5/2}$), they lead to very significant variations of the kinetic energy over a short period, after turbulence has entered its ultimate dissipative regime. This demonstrates how the sudden dissipation effect can introduce an enormous sensitivity to initial conditions in turbulent plasma under compression.

5 Summary

In this work, a statistical two-point EDQNM model has been proposed to predict the evolution of turbulent plasma under compression and to account for sudden dissipation effects due to the increase of viscosity. The model's results are in very good qualitative and quantitative agreement with results from Direct Numerical Simulations. The model permits parametric studies, and to reach higher Reynolds numbers than DNS. By considering different scalings of the infrared range in the initial spectrum, we demonstrate the importance of the initial distribution of energy at large scales, for different cases of Batchelor- and Saffman-type turbulence. We show that modifications in the initial conditions induce significant differences of energy level during the sudden dissipation phases, and in the later stage of turbulence decay. As expected from theoretical scaling arguments, the larger the energy at large scales, the smaller the decay rates. A self-similar analysis of the sudden dissipation effects also allows to understand this phenomenon and to quantify it by identifying the different scaling laws that appear in the turbulent kinetic energy decay.

Références

[1] Davidovits, S., Fisch, N. J. (2016). Sudden viscous dissipation of compressing turbulence. Physical review letters, 116(10), 105004.

[2] Gréa, B. J., Griffond, J., Burlot, A. (2014). The effects of variable viscosity on the decay of homogeneous isotropic turbulence. Physics of Fluids, 26(3), 035104.

[3] Lindl, J. (1995). Development of the indirect drive approach to inertial confinement fusion and the target physics basis for ignition and gain. Physics of Plasmas, 2(11), 3933-4024.

[4] Godeferd, F. S., Cambon, C. (1994). Detailed investigation of energy transfers in homogeneous stratified turbulence. Physics of Fluids, 6(6), 2084-2100.

[5] Sagaut, P., Cambon, C. (2008). Homogeneous turbulence dynamics (Vol. 10). Cambridge : Cambridge University Press.

[6] Lesieur, M. and Ossia, S.,(2000), 3D isotropic turbulence at very high Reynolds numbers : EDQNM study, Journal of Turbulence, 1, 1-25

[7] Burlot, A. and Gréa, B.-J. and Godeferd, F. S. and Cambon, C. and Soulard, O., (2015), Large Reynolds number self-similar states of unstably stratified homogeneous turbulence, Physics of Fluids, 27 (6), 065114.

[8] Cambon, C., Mao, Y., Jeandel, D. (1992). On the application of time dependent scaling to the modelling of turbulence undergoing compression. European Journal of Mechanics B Fluids, 11, 683-703.